Desalination and Water Treatment
www.deswater.com

doi: 10.5004/dwt.2019.23728

150 (2019) 274–281
May

Adsorption behavior of tungstate on montmorillonite as a function of pH, ionic strength and competitive anion

Ruiping Li[a,b,*], Yunmeng Tang[a], Xin Li[a], Caijin Tang[a], Yuxiang Zhu[b], Shiliang Wang[a], Chunye Lin[b,*]

[a]*School of geography and tourism, Qufu Normal University, Qufu, China, Tel. +86 10 3980705; emails: liruiping858@163.com (R.P. Li), ymt970423@163.com (Y.M. Tang), LeeXin97@163.com (X. Li), tangcaijin124@163.com (C.J. Tang), sdqfsf@163.com (S.L. Wang)*
[b]*State Key Joint Laboratory of Environmental Simulation and Pollution Control, School of Environment, Beijing Normal University, Beijing, China, Tel./Fax: +86 10 58801858; emails: c.lin@bnu.edu.cn (C.Y. Lin), zhuyuxiang@mail.bnu.edu.cn (Y.X. Zhu)*

Received 10 September 2018; Accepted 31 December 2018

ABSTRACT

A better understanding of adsorption mechanism is vital for the effective reduction of tungsten mobility and potential human health risk such as its suspected link to the childhood leukemia clusters. This study investigated tungstate (WO_4^{2-}) adsorption characteristic onto montmorillonite under environmentally relevant solution properties such as the influence of reaction time, solution pH, initial concentration, the competitive anion (PO_4^{3-}), and ionic strength. The results of the adsorption isotherm studies suggested that both the Langmuir (R^2 = 0.9117) and Freundlich (R^2 = 0.9913) equations can be well consistent with WO_4^{2-} adsorption process and the maximal WO_4^{2-} adsorption capacity was 26.73 mmol kg^{-1}. The amount of WO_4^{2-} adsorbed onto montmorillonite strongly dependent on pH and slightly dependent on ionic strength. Specifically, WO_4^{2-} adsorption reached the maximum (17.41 mmol kg^{-1}) at pH 4.15, but becoming negligible (<10%) when pH increase above 9. PO_4^{3-} competed for adsorption sites on montmorillonite with WO_4^{2-}. The results of this study indicated that the adsorption mechanism of WO_4^{2-} onto montmorillonite involved ion exchange, inner-sphere surface complexation reaction, and electrostatic attraction. Collectively, our study will aid the understanding of tungsten fate and these results suggest that montmorillonite can be advantageous to the adsorption and recovery of tungsten from real wastewater.

Keywords: Montmorillonite; Tungstate; Adsorption

1. Introduction

Recently, The geochemistry and fate of tungsten has recently gained interest in the scientific and regulatory communities because of its suspected link to the childhood leukemia clusters recently discovered in Nevada, Arizona and California [1–3]. Although, it is no clear evidence that increased concentrations of tungsten leads to these childhood leukemia clusters, much research has recognized that tungsten may be carcinogenic to mammals and toxic to organisms [4–6]. Then, tungsten (*W*) has been recently identified as an emerging environmental contaminant by the United States Environmental Protection Agency (US EPA) [7].

China is the world's largest *W* producer and consumer. In 2016, the global production of tungsten was 86,400 ton, with over 86% of tungsten (71,000 ton) being produced in China [8]. We have found *W* mining activity in China has contaminated the nearby agricultural soil and led to *W* bioaccumulation in the rice [9]. As anthropogenic activities result in massive amounts of tungsten being released into the environment systems [2], enriching our knowledge of the migration and transformation of *W* in the environmental interfaces is necessary.

* Corresponding authors.

Tungsten persists as tungstate anion or, via polymerization, as a variety of poly-tungstate species, each with varying solubility and soil sorption characteristics [1,3–4,10]. The adsorption behavior of tungsten with soils and clay minerals is the major migration process by which tungsten can be migrated and redistributed in the environment, a comprehensive study of the adsorption mechanism plays an important role in understanding tungsten fate and to remediate tungsten pollution in the environment [10,11].

Montmorillonite is important sink for many oxyanions in the environment and have already been reported to adsorb tungsten (VI) effectively [12,13]. However, existing data for W (VI) adsorption on montmorillionite are relatively limited and incomplete. Hence, the purpose of this research is to investigate the adsorption mechanism of W (VI) onto montmorillonite across varying the solution pH, ionic strength, contact time, initial WO_4^{2-} concentration and competitive anion (PO_4^{3-}). This fundamental study will be helpful for the treatment of soil and water contaminated by tungsten industries and mining.

2. Materials and methods

2.1. Materials and regents

All chemicals used in this study were of analytical grade or higher and used without further purification. Double distilled water was used to prepare solution and clean the sample bottle. All samples were performed in duplicate.

Montmorillonite was obtained from Sigma-Aldrich. Adsorbent properties were characterized by the following methods. X-ray diffraction (XRD) analysis was carried out by a X'Pert PRO MPD machine (PANalytical B.V., Netherlands) with filtered Cu Kα radiation (n = 0.1548 nm) operated at 40 kV and 40 mA. Fourier Transform Infrared (FTIR) was performed using a Fourier infrared instrument (Nicolet Nexus 670, America) in pressed KBr pellets. The spectral resolution was sent to 4 cm^{-1}, and 32 scans were collected for each spectrum. The specific surface area (SSA) was surved by the Model QS-7 Quantasorb surface area analyzer (Quantachrom Co., Greenvale, NY).

2.2. Adsorption experiments

The specific experimental steps for WO_4^{2-} adsorption onto montmorillionite and analytical Instruments have been previously reported [14–15]. The detailed experimental parameters list in Table 1. The standard deviation of samples was generally less than 5%.

3. Results and discussion

3.1. Characterization of montmorillonite

Fig. 1 shows the XRD patterns of montmorillonite sample. The structure of montmorillonite sample is given as $Al_2O_9Si_3$. The peak appears at 26.62 (2θ) indicates impurity corresponding to quartz in this montmorillonite mineral. The FT-IR spectrum of montmorillonite sample is shown in Fig. 2. The adsorption band at 3,620 cm^{-1} is due to stretching vibrations of structural –OH groups of montmorillonite. Water in montmorillonite shows strong absorption at 3,440 cm^{-1} and near 1,638 cm^{-1} region due to the H_2O-stretching and bending vibrations, respectively [16]. A sharp band at 796 cm^{-1} confirms quartz admixture in the sample. The very strong adsorption band at 1,089 cm^{-1} with inflexion near 1,039 cm^{-1}

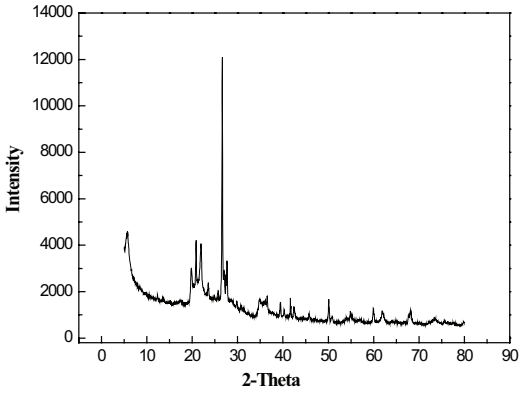

Fig. 1. XRD pattern of montmorillonite sample.

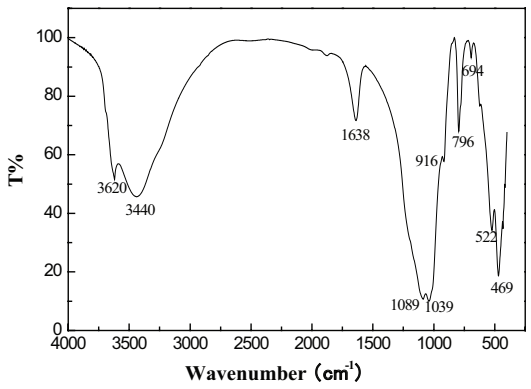

Fig. 2. FTIR spectrum of montmorillonite sample.

Table 1
Experimental conditions of tungstate adsorption onto the montmorillonite

Experiment	pH	Ionic strength (M NaCl)	Initial *W* concentration (mM)	Equilibrating time (h)
Kinetic	5.0	0.1	0.54	1–60
Isotherm	5.0	0.1	0.08–1.63	48
pH influence	3–11	0.1	0.54	48
Ionic strength influence	5.0	0.001, 0.005, 0.01,0.05, 0.1	0.54	48
Competitive anion influence	5.0	0.1	0.54	48

is due to Si-O bending vibration [16,17]. The band at 916 cm^{-1} is related to Al-Al-OH bending vibrations. The band at 694 cm^{-1} is due to the deformation and bending modes of the Si-O groups, while the bands at 522 and 469 cm^{-1} are resulted from Al-O-Si and Si-O-Si bending vibration, respectively [17]. Finally, the SSA of the montmorillonite is 103.85 $m^2\ g^{-1}$ determined by BET method using N_2.

3.2. Adsorption kinetics of WO_4^{2-} onto montmorillonite

Kinetic study results of WO_4^{2-} adsorption onto montmorillonite is shown in Fig. 3. WO_4^{2-} exhibited rapid reaction during the first 48 h and the reaction rate decreased becoming asymptotic to the time axis after 48 h. Therefore, 48 h was selected as the equilibrium time for WO_4^{2-} adsorption onto montmorillonite. Rapid reaction is often interpreted by scholars as high-affinity sites, while slow reaction as intra-particle diffusion into the mineral defects, the precipitation of ion on the mineral surface, or lower reactive sites [18]. Similar kinetic profile was found for WO_4^{2-} adsorption onto kaolinite [15].

The kinetic data were simulated with three models: the pseudo-first-order and pseudo-second-order model [19], and the intra-particle diffusion model [20]. The kinetic formula is expressed by the following equations, for the pseudo-first-order model:

$$\log\left(q_e - q\right) = \log q_e - \frac{k_1}{2.303}t \tag{1}$$

The pseudo-second-order model:

$$\frac{t}{q} = \frac{1}{k_2 q_e^2} + \frac{1}{q_e}t \tag{2}$$

The intra-particle diffusion model:

$$q = k_{id}t^{1/2} + C \tag{3}$$

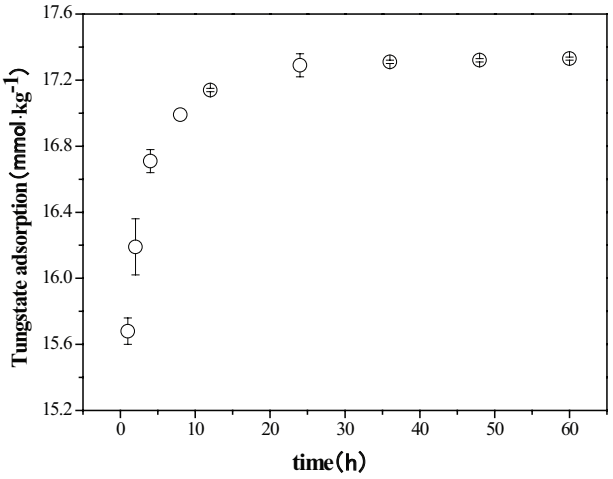

Fig. 3. Influence of reaction time on the tungstate adsorption onto montmorillonite, I = 0.1 M NaCl, pH = 5.0 ± 0.1, T = 25°C ± 2°C, and $C_{\text{tungstate initial}}$ = 0.54 mM.

In Eqs. (1)–(3), q and q_e (mmol kg^{-1}) are the amounts of WO_4^{2-} adsorbed at the time, t (h) and at equilibrium, respectively, k_1 (h^{-1}) is the pseudo-first-order rate constant for WO_4^{2-} adsorption, k_2 (kg $mmol^{-1}$ h^{-1}) is the pseudo-second-order rate constant (kg $mmol^{-1}$ h^{-1}), k_{id} (mmol kg^{-1} $h^{-1/2}$) is the relevant rate constant for WO_4^{2-} adsorption and C is the intercept.

Plots of the three kinetic model of WO_4^{2-} adsorption onto montmorillonite are presented in Fig. 4. Comparing with the pseudo-first-order model, the diagram of t/q_t vs. t (Fig. 4(b))

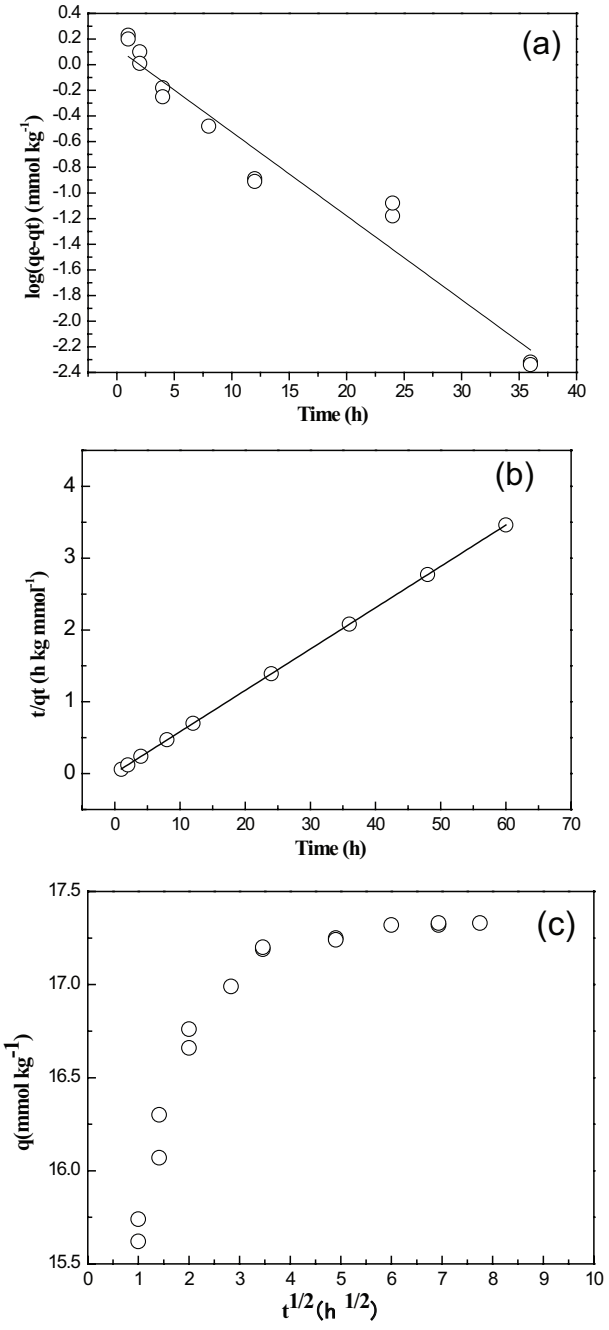

Fig. 4. Kinetic simulation of tungstate adsorption onto montmorillonite: (a) the pseudo-first-order model, (b) the pseudo-second order model, (c) the intra-particle diffusion model.

indicates that the pseudo-second-order model (R^2 = 0.999) will better simulate the kinetics of WO_4^{2-} adsorption onto montmorillonite than pseudo-first-order model (R^2 = 0.944). Value of k_1 calculated from linear graph was 1.38 × 10^{-2} h^{-1}, which is similar with WO_4^{2-} adsorption onto Oxisols (K_{ad} 1.10 × 10^{-2} h^{-1} at the initial WO_4^{2-} concentration 0.04 mM) [15] and kaolinite (K_{ad} 1.05 × 10^{-2} h^{-1} at the initial WO_4^{2-} concentration 0.27 mM) [14]. The value of k_1 was varied with different initial WO_4^{2-} concentration and different materials. Plot of q vs. $t^{1/2}$ (Fig. 4(c)) followed three distinct phases of adsorption process, initial curved portion followed by linear and a plateau. The initial curved portion is resulted from the bulk diffusion, the linear portion of the solid-state diffusion and the plateau to the relative equilibrium. The properties of graph show that the uptake of WO_4^{2-} by montmorillonite is controlled by surface adsorption and intra-particle diffusion. The rate constants value (k_{id}) obtained from the slope of the linear portion of the curve was 0.171 mmol kg^{-1} $h^{1/2}$.

3.3. Adsorption isotherm

The adsorption process of WO_4^{2-} onto montmorillonite was modeled by the Langmuir and Freundlich equation. The Langmuir model [21] assumes that monolayer adsorption occurs on a finite number of homogenous surfaces without any interaction between adsorbed ions, and the equation is represented by the following:

$$\frac{C_e}{q_e} = \frac{C_e}{q_m} + \frac{1}{q_m K_L} \tag{4}$$

where C_e (mmol L^{-1}) is the equilibrium concentration of WO_4^{2-} in solution, q_e (mmol kg^{-1}) is the WO_4^{2-} adsorption amount, q_m (mmol kg^{-1}) is the maximal adsorption capacity, and K_L (L $mmol^{-1}$) is the constant related to the binding energy.

The Freundlich isotherm [22] is commonly used for heterogeneous, multilayer adsorption, and the equation can be expressed as:

$$q_e = K_F C_e^{1/n} \tag{5}$$

where C_e (mmol L^{-1}) is the equilibrium concentration of WO_4^{2-} in solution, q_e (mmol kg^{-1}) is the WO_4^{2-} adsorption amount, K_F ($mmol^{1-n}$ kg^{-1} L^n) is the Freundlich constant related to the adsorption intensity, and n is the heterogeneity factor.

Fig. 5 shows the adsorption isotherms of WO_4^{2-} onto montmorillonite and fits of the Langmuir and Freundlich equation. Based the correlation coefficients, the Freundlich isotherm describes the experimental data better than Langmuir equation (Table 2). The WO_4^{2-} maximal adsorption capacity was 26.73 mmol kg^{-1} and equilibrium constant K_L = 0.0793 L $mmol^{-1}$, which was consistent with the previous research [12,13,23]. Tuna and Braida [12] found the maximal predicted WO_4^{2-} capacity of montmorillonite was 9.89 mmol kg^{-1}. We believed experimental conditions and the different characteristic of adsorbent can account for this discrepancy. Our previous research founded that both the Langmuir model and the Freundlich model were fitted to the WO_4^{2-} adsorption onto the Oxisols, which the maximal adsorption capacity of WO_4^{2-} was 10.09 mmol kg^{-1} and the distribution coefficient 12.6 L g^{-1} [15]. Xu et al. [24] found that goethite adsorbed more tungstate than montmorillonite with the maximal capacity of 225.7 mmol kg^{-1} and the distribution coefficient 159.1 L g^{-1}. The difference of montmorillonite characteristics (i.e. specific surface area, surface charges) leads to varies of the maximum WO_4^{2-} adsorption amount.

3.4. Effect of pH

Solution pH can affect the adsorption of WO_4^{2-} onto montmorillonite through multiple pathways such as affecting surface site protonation, and WO_4^{2-} complexation and hydrolysis. Effect of pH on the adsorption of WO_4^{2-} onto montmorillonite is illustrated in Fig. 6. As shown in the figure, it is clear that the amount of adsorbed WO_4^{2-} decreased with increasing solution pH. More specifically, the amount of adsorbed WO_4^{2-} reached the maximum (17.41 mmol kg^{-1}) at equilibrium pH around 4.15, decreased steadily in the pH range from 5.0 to 7.0 and became negligible (<10%) when pH increase above 9.0. This is consistent with previous study that WO_4^{2-} adsorption is pH dependent with increased adsorption occurring at acidic pH and little at pH > 9 [12,25]. One possible explanation is the protonation state of clay surface functional groups. Also, the aqueous speciation of tungsten changes with pH is also another issue, which is influenced by the pKa

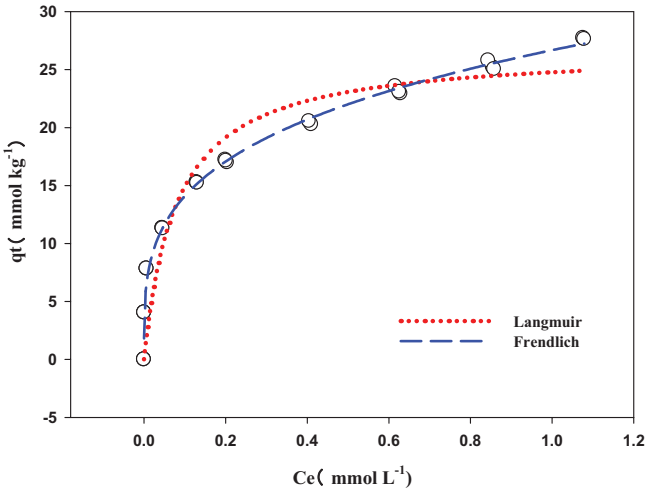

Fig. 5. Adsorption isotherm of tungstate onto montmorillonite clay, I = 0.1 M NaCl, pH = 5.0 ± 0.1, T = 25°C ± 2°C, and $C_{tungstate\ initia}$ = 0.08 to 1.63 mM.

Table 2
Langmuir and Freundlich constants of tungstate adsorption on montmorillonite

Model	Langmuir	Freundlich
K_L, L $mmol^{-1}$	0.0793	—
Q_{max}, mmol kg^{-1}	26.73	—
K_F, $mmol^{1-n}$ kg^{-1} L^n	—	26.68
N	—	3.60
R^2	0.9117	0.9913
SE	2.93	0.92

value [26]. The two pKa values for H_2WO_4 (pKa1 = 3.62 [27], pKa2 =5.08 [28]) bracket a wider pH range which promotes the adsorption of WO_4^{2-} on montmorillonite. The dimeric tungstate ions (WO_4^{2-}) occurs in alkaline environemnts, whereas a number of thermodynamically stable and unstable polymerized tungstate forms coexist in acidic solution as in Fig. 7 [1,29–31]. Some microscopic spectral evidences (i.e. XAS and ATR-FTIP) for the effect of pH on WO_4^{2-} speciation change have been reported [11,31,32]. Specifically, the formation of polymeric of WO_4^{2-} under a wide pH range (i.e. pH 4–8) decreased the WO_4^{2-} adsorption amount on mineral surface, and thereby led to easily tungsten mobilization in the environment [11,31,32]. Another possible explanation is that an increase of OH^- ions in basic solution will compete with WO_4^{2-} for the adsorption sites and result in a decrease in WO_4^{2-} adsorption. So the adsorption mechanism of WO_4^{2-} onto montmorillonite involves more than one mechanism such as polymerization at low pH and adsorption.

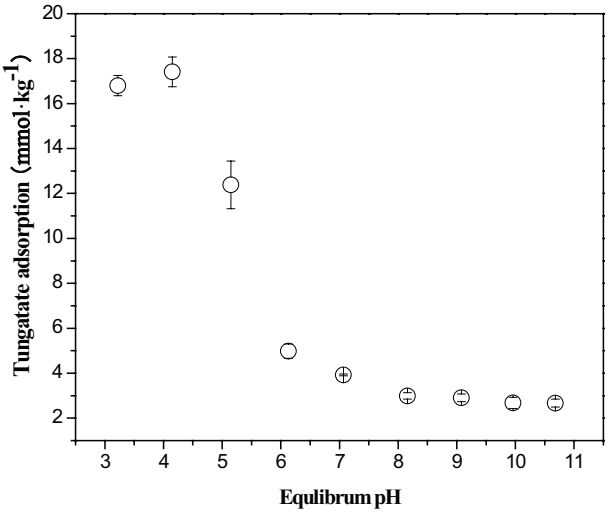

Fig. 6. Influence of pH on tungstate adsorption onto the montmorillonite, I = 0.1 M NaCl, pH = 3.0 ± 0.1 to 11 ± 0.1, T = 25°C ± 2°C, and $C_{\text{tungstate initial}}$ = 0.54 mM.

Positive identification of adsorbed WO_4^{2-} species was provided using the XRD and FTIR technique. In Fig. 8(a) XRD pattern is presented for the sorbent, as well as for the sorbent after WO_4^{2-} sorption at pH 5.0. Following WO_4^{2-} sorption, the loaded sorbent had the same structure of montmorillonite. But three new bands appearing at 20°, 26°, and 50° could be attributed to the formation of new precipitate, which indicates surface complexation. FTIR spectrophotometer result of montmorillonite, both before and after WO_4^{2-} adsorption, shows several frequency shifts (Fig. 8(b)).These shifts are important indicators of molecular interactions and reflect the effect of the surface complexation between adsorption sites and WO_4^{2-} species rather than solid phase precipitation.

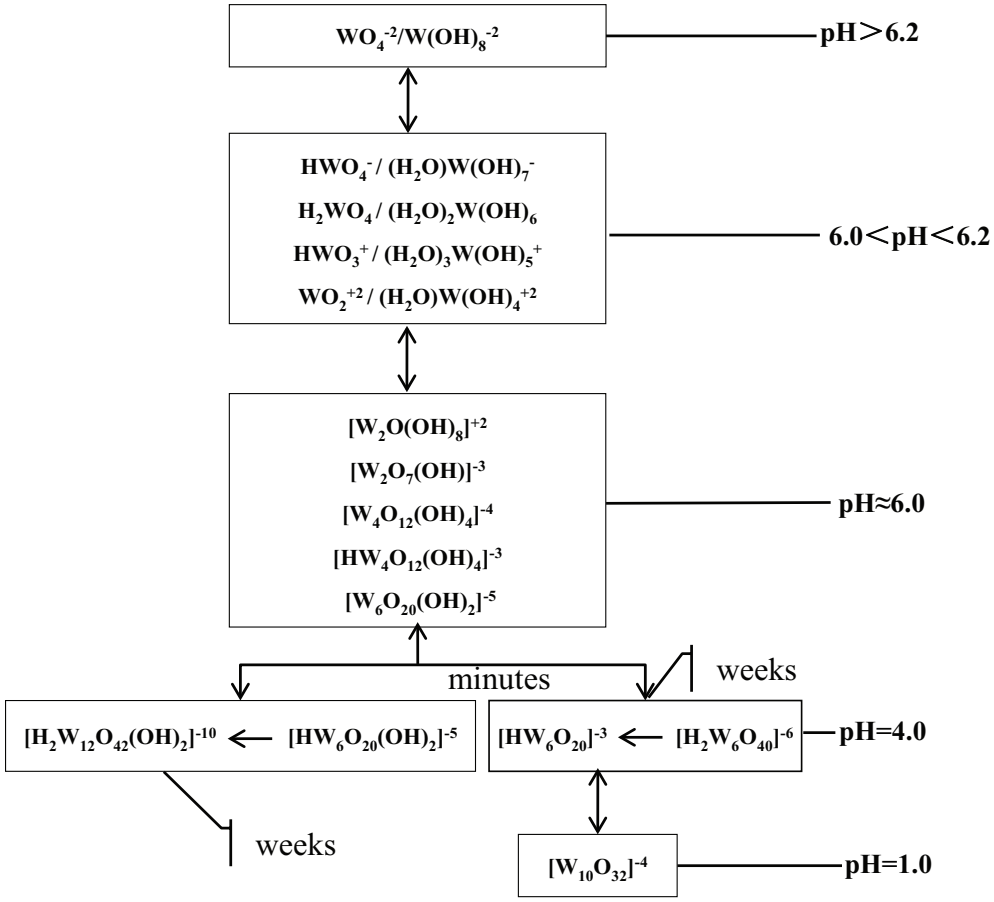

Fig. 7. Tungsten speciation as a function of pH (based on references [1,29–31]).

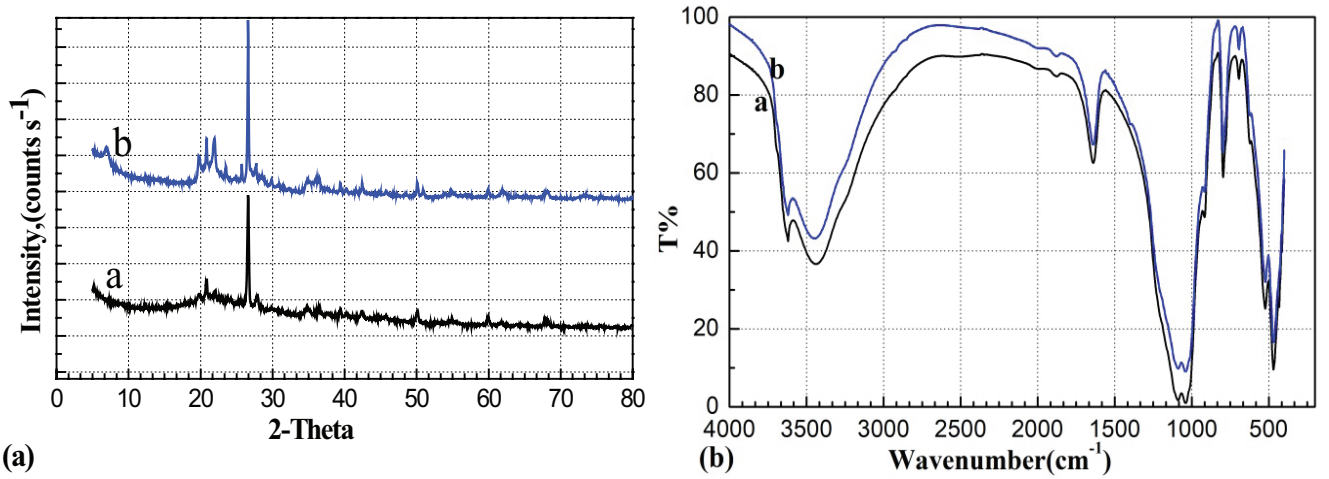

Fig. 8. (a) X-ray patterns of montmorillonite and montmorillonite after tungstate adsorption, (b) FTIR spectra of montmorillonite and montmorillonite after tungstate adsorption.

3.5. Effect of ionic strength

Ionic strength plays a role in the WO_4^{2-} adsorption onto montmorillonite (Fig. 9.). It was illustrated that the amount of adsorbed increased steadily from 35.2% to 62.0% with the increase of ionic strength. One definitive explanation is that the increase of solution ionic strength for clay systems results in the shielding of the net negatively-charged surface electric field, and thereby reduce the repulsive force to anion [34,35]. This effect allows more WO_4^{2-} to adsorb onto the montmorillonite surface at high ionic strength conditions as compared with low ionic strength conditions. Another possible explanation is the formation of inner-sphere WO_4^{2-} surface complexes, because higher ionic strength may facilitate the transformation of outer-sphere complex into inner-sphere complex and hence might increase total adsorption amount [33]. Increased WO_4^{2-} adsorption at high ionic strength is consistent with previous research of WO_4^{2-} adsorption onto pyrite and boehmite, where it was suggested that the increased WO_4^{2-} adsorption may be caused by the effect of coadsorption of cations (i.e., Na^+) and WO_4^{2-} [11,36]. Thus, the effect of ionic strength for WO_4^{2-} adsorption onto the clay colloid surface may include the promotion of the inner-sphere adsorption process and the weakness of the positive electrostatic field at the mineral surface and finally increased the total WO_4^{2-} adsorption.

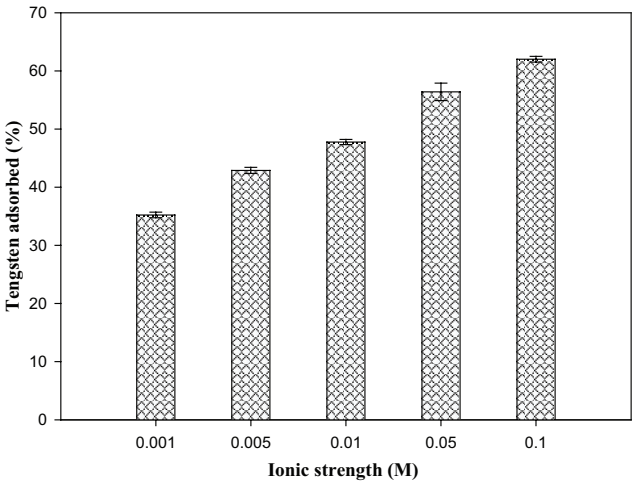

Fig. 9. Influence of ionic strength on tungstate adsorption onto the montmorillonite, I = 0.001 to 0.1 M NaCl, pH = 5.0 ± 0.1, T = 25°C ± 2°C, and $C_{\text{tungstate initial}}$ = 0.54 mM.

3.6. Effect of competitive anions

The influence of competitive anion PO_4^{3-} on the adsorption of WO_4^{2-} onto montmorillonite was investigated using the mol ratio P/W from 0 to 10 (Fig. 10). As shown in Fig. 10, tungstate adsorption onto montmorillonite was strongly affected by phosphate. Without adding phosphate, the amount of adsorbed WO_4^{2-} was 15.83 mmol kg^{-1}, but the adsorption of WO_4^{2-} gradually decreased with the increase of the phosphate concentration. However, the final decrease amount of adsorbed WO_4^{2-} (14.30 mmol kg^{-1}) is less than the final increase amount of adsorbed PO_4^{3-} (113.30 mmol kg^{-1}) with the change of the mol ratio P/W

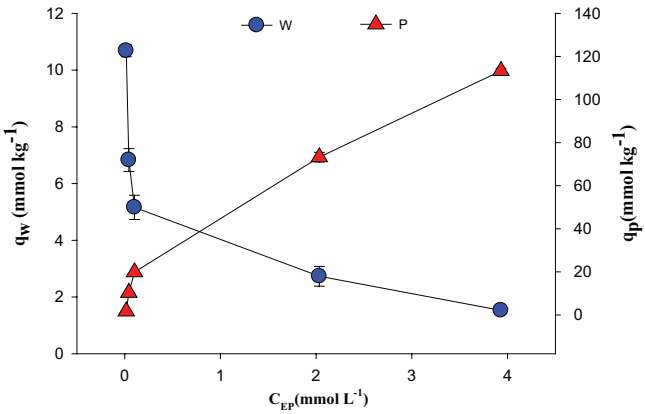

Fig. 10. Influence of phosphate on the adsorption of tungstate. I = 0.1 M NaCl, pH = 5.0 ± 0.1, T = 25°C ± 2°C, $C_{\text{tungstate initial}}$ = 0.5 mM, and $C_{\text{phosphate}}$ = 0.05 to 5.0 M.

from 0 to 10, which suggesting that the specific adsorption of WO_4^{2-} onto montmorillonite surface and the stronger affinity of montmorillonite for PO_4^{3-} compared with the affinity for WO_4^{2-}. Mulcahy et al., [37] concluded that alumina contained loosely and tightly bound surface sites for WO_4^{2-} adsorbed. Therefore, it can be explained that the montmorillonite might have small adsorption sites common to WO_4^{2-} and PO_4^{3-} anions and large adsorption species specific to WO_4^{2-} or PO_4^{3-} anions. PO_4^{3-} affecting adsorption of WO_4^{2-} by competing for a few percent available surface sites has been reported on natural soil and other minerals (such as ferrihydrite, kaolinite and oxisols) [15,38]. Another interpretation for the decreased adsorption of WO_4^{2-} is that WO_4^{2-} polymerizes with PO_4^{3-} and produces polyoxometalates (POMs) such as phosphotungstate $PW_{12}O_{40}^{3-}$ in solution [31]. So PO_4^{3-} reduces WO_4^{2-} adsorption onto montmorillonite by competing for limited surface adsorption sites and altering the WO_4^{2-} solution speciation in solution.

4. Conclusion

Recently, interest in tungsten (*W*) geochemistry and transformation has increased due to its suspected link to the childhood leukemia clusters. A comprehensive understanding of adsorption mechanism is vital for the effective reduction of tungsten mobility and potential human health risk. However, existing data are relatively limited and incomplete. In this study, the results have confirmed that tungstate adsorption onto montmorillonite is an important factor influencing the tungsten transformation in natural environments. Montmorillonite can be used as an important scavenger for removing of tungsten from aqueous solution by adsorption process. Specifically, the kinetic adsorption data of tungstate onto montmorillonite was well simulated by a pseudo-second-order model and suggested the rate-controlling steps of tungstate was intra-particle diffusion and rapid out-sphere adsorption. The adsorption isotherm data was fitted into both Langmuir and Freundlich model. The amount of tungstate adsorption onto montmorillonite decreased with pH increasing but increased with ionic strength. Phosphate competed with tungstate for adsorption sites onto montmorillonite. These results demonstrate that the mechanism for tungstate adsorbed onto montmorillonite was electrostatic attraction and inner-sphere surface complexation reaction and influenced by many factors such as intrinsic properties of adsorbent, tungsten concentration, and speciation, solution pH, ionic strength, and the reaction time. This study investigated a single adsorbent and simple composition of solutions. The natural environment is a very complex system, which could complicate the transformation and migration of *W* in environment. Further efforts are required to improve knowledge of W environmental chemistry, and its environmental transformation and exposure.

Acknowledgements

This study was supported by the National Natural Science Foundation of China (41371441) and College Students Innovation and Entrepreneurship Training Program (201810446039).

Reference

[1] A. Koutsospyros, W. Braida, C. Christodoulatos, D. Dermatas, N. Strigul, A review of tungsten: from environmental obscurity to scrutiny, J. Hazard Mater., 136 (2006) 1–19.
[2] R. L. Seiler, K.G. Stollenwerk, J.R. Garbarino, Factors controlling tungsten concentrations in ground water, Carson Desert, Nevada. App. Geochem., 20 (2005) 423–441.
[3] P.R. Sheppard, G. Ridenour, R.J Speakman, M.L. Witten, Elevated tungsten and cobalt in airborne particulates in Fallon, Nevada: possible implications for the childhood leukemia cluster, Appl. Geochem., 21 (2006) 152–165.
[4] N. Strigul, A. Koutsospyros, P. Arienti, C. Christodoulatos, D. Dermatas, W. Braida, Effects of tungsten on environmental systems, Chemosphere, 61 (2005) 248–258.
[5] A.D. Kelly, M. Lemaire, Y.K. Young, J.H. Eustache, C. Guilbert, M.F. Molina, K.K. Mann, In vivo tungsten exposure alters B-cell development and increases DNA damage in murine bone marrow, Toxicol. Sci., 131 (2013) 434–446.
[6] I.D.S. Adamakis, E. Panteris, E.P. Eleftheriou, Tungsten toxicity in plants, Plants, 1 (2012) 82–99.
[7] EPA, Emerging-Contaminant–Tungsten (Fact Sheet (2008). U.S. EPA (EPA 505-F-07–005)), 2008
[8] K.B. Shedd, Tungsten. In: Mineral Commodity Summaries. U.S.Geol. Surv., 2017.
[9] C.Y. Lin, R.P. Li, H.G. Cheng, J. Wang, X. Shao, Tungsten distribution in soil and rice in the vicinity of the world's largest and longest-operating tungsten mine in China, PloS one, 9 (2014) e91981.
[10] J.P. Gustafsson, Modelling molybdate and tungstate adsorption to ferrihydrite, Chem. Geol., 200 (2003) 105–115.
[11] H. Hur, R.J. Reeder, Tungstate sorption mechanisms on boehmite: systematic uptake studies and X-ray absorption spectroscopy analysis, J. Colloid Interface Sci., 461 (2016) 249–260.
[12] G.S. Tuna, W. Braida, Evaluation of the adsorption of mono- and polytungstates onto different types of clay minerals and Pahokee peat, Soil Sedim. Contam. Int. J., 23 (2014) 838–849.
[13] G. S. Tuna, W. Braida, A. Ogundipe, D. Strickland, Assessing tungsten transport in the vadose zone: from dissolution studies to soil columns, Chemosphere, 86 (2012) 1001–1007.
[14] R.P. Li, C.Y. Lin, X.T. Liu, Adsorption of tungstate on kaolinite: adsorption models and kinetics, RSC Adv., 6 (2016) 19872–19877.
[15] R.P. Li, R.N. Luan, C.Y. Lin, D.Q. Jiao, B.B. Guo, Tungstate adsorption onto oxisols in the vicinity of the world's largest and longest-operating tungsten mine in China, RSC Adv., 4 (2014) 63875–63881.
[16] J. Madejová, M. Janek, P. Komadel, H.J. Herbert, H. Moog, FTIR analyses of water in MX-80 bentonite compacted from high salinary salt solution systems, Appl. Clay Sci., 20 (2002) 255–271.
[17] H. Zaitan, D. Bianchi, O. Achak, T. Chafik, A comparative study of the adsorption and desorption of o-xylene onto bentonite clay and alumina, J. Hazard Mater., 153 (2008) 852–859.
[18] L. Axe, P.R. Anderson, Experimental and theoretical diffusivities of Cd and Sr in hydrous ferric oxide, J. Colloid Interface Sci., 185 (1997) 436–448.
[19] S. Lagergren, About the theory of so-called adsorption of soluble substances, K. Sven. Vetensk.akad. Handl, 24 (1898) 1–39.
[20] W. Weber, J. Morris, Kinetics of adsorption on carbon from solution, J. Sanit. Eng. Div. Am. Soc. Civ. Eng., 89 (1963) 31–60.
[21] I. Langmuir, The adsorption of gases on plane surfaces of glass, mica and platinum, J. Am. Chem. Soc., 40 (1918) 1361–1403.
[22] H.M.F.Z. Freundlich, The adsorption in physical chemistry, Phys. Chem., 57 (1906) 385–470.
[23] D. Dermatas, W. Braida, C. Christodoulatos, N. Strigul, N. Panikov, M. Los, S. Larson, Solubility, sorption, and soil respiration effects of tungsten and tungsten alloys, Environ. Forensics, 5 (2004) 5–13.
[24] N. Xu, C. Christodoulatos, A. Koutsospyros, W. Braida, Competitive sorption of tungstate, molybdate and phosphate mixtures onto goethite, Land Contam. Reclam., 17 (2009) 45–57.
[25] N. Xu, C. Christodoulatos, W. Braida, Modeling the competitive effect of phosphate, sulfate, silicate, and tungstate anions on the

adsorption of molybdate onto goethite, Chemosphere, 64 (2006) 1325–1333.
[26] F.J. Hingston, A.M. Posner, J.P. Quirk, Competitive adsorption of negatively charged ligands on oxide surfaces., Discuss. Faraday Soc., 52 (1971) 334–342.
[27] D. Wesolowski, S.E. Drummond, R.E. Mesmer, H. Ohmoto, Hydrolysis equilibria of tungsten (VI) in aqueous sodium chloride solutions to 300 degree, Inorg. Chem., 23 (1984) 1120–1132.
[28] S.A. Wood, I.M. Samson, The hydrothermal geochemistry of tungsten in granitoid environments: i. Relative solubilities of ferberite and scheelite as a function of T, P, pH, and mNaCl, Econ. Geol., 95 (2000) 143–182.
[29] H. Gecol, P. Miakatsindila, E. Ergican, S.R Hiibel, Biopolymer coated clay particles for the adsorption of tungsten from water, Desalination, 197 (2006) 165–178.
[30] E. Lassner, W.D. Schubert, Tungsten: Properties, Chemistry, Technology of the Element, Alloys, and Chemical Compounds, Springer: New York, 1999.
[31] J. Sun, B.C. Bostick, Effects of tungstate polymerization on tungsten(VI) adsorption on ferrihydrite, Chem. Geol., 417 (2015) 21–31.
[32] S. Rakshit, B. Sallman, A. Davantes, G. Lefevre, Tungstate (VI) sorption on hematite: an in situ ATR-FTIR probe on the mechanism, Chemosphere, 168 (2017) 685–691.
[33] M.B. McBride, A critique of diffuse double layer models applied to colloid and surface chemistry, Clay Clay Miner., 45 (1997) 598–608.
[34] A.M.L. Kraepiel, K. Keller, F.M.M. Morel, On the acid-base chemistry of permanently charged minerals, Environ. Sci. Technol., 32 (1998) 2829–2838.
[35] W.D. Hao, S.L. Flynn, D.S. Alessi, K.O. Konhauser, Change of the point of zero net proton charge (pH_{PZNPC}) of clay minerals with ionic strength, Chem. Geol., 493 (2018) 458–467.
[36] M. Cui, K.H. Johannesson, Comparison of tungstate and tetrathiotungstate adsorption onto pyrite, Chem. Geol., 464 (2017) 57–68.
[37] F.M. Mulcahy, M.J. Fay, A. Proctor, M. Houalla, D.M. Hercules, The adsorption of metal oxyanions on alumina, J. Catal., 124 (1990) 231–240.
[38] T. Iwai, Y. Hashimoto, Adsorption of tungstate (WO_4) on birnessite, ferrihydrite, gibbsite, goethite and montmorillonite as affected by pH and competitive phosphate (PO_4) and molybdate (MoO_4) oxyanions, App. Clay Sci., 143 (2017) 372–377.